LBL-30571
UC-404
Preprint

Lawrence Berkeley Laboratory
UNIVERSITY OF CALIFORNIA

Materials Sciences Division

Submitted to Electrochimica Acta

The Effect of Surface Reconstruction on the Capacitance of Au(100) Surfaces

P.N. Ross and A.T. D'Agostino

April 1991

For Reference

Not to be taken from this room

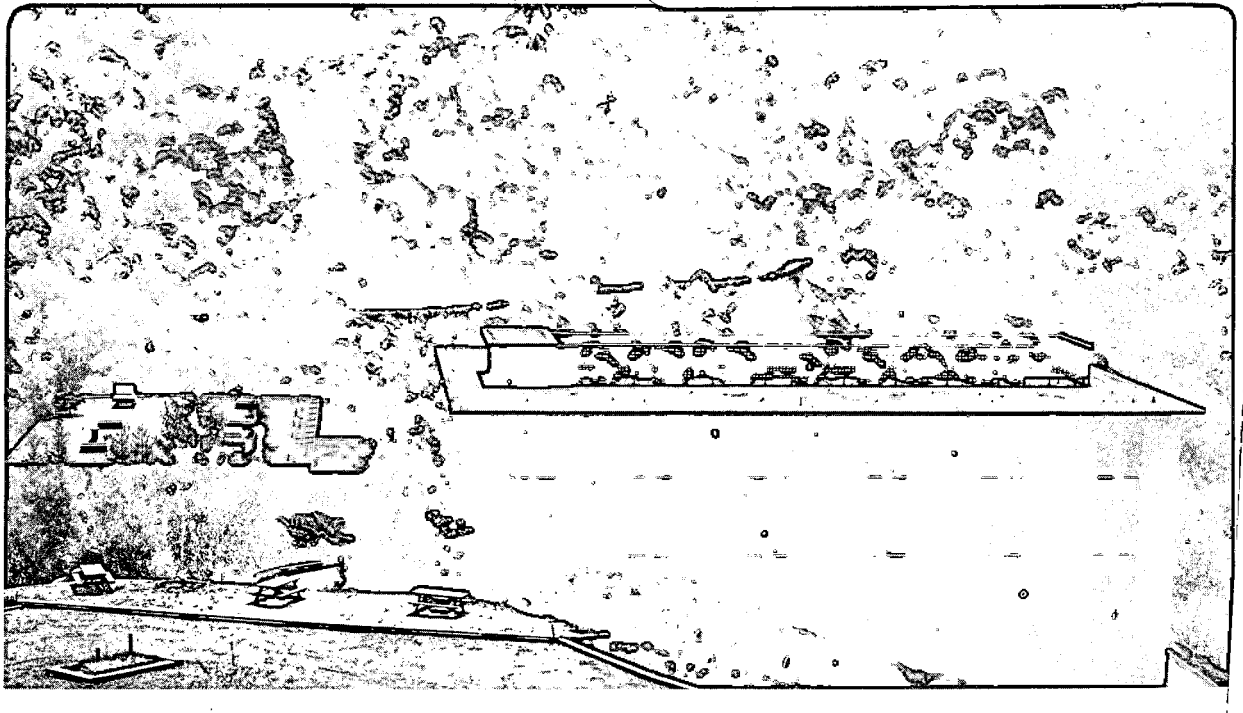

Prepared for the U.S. Department of Energy under Contract Number DE-AC03-76SF00098

LBL-30571
Copy 1
Bldg. 50 Library.

DISCLAIMER

This document was prepared as an account of work sponsored by the United States Government. Neither the United States Government nor any agency thereof, nor The Regents of the University of California, nor any of their employees, makes any warranty, express or implied, or assumes any legal liability or responsibility for the accuracy, completeness, or usefulness of any information, apparatus, product, or process disclosed, or represents that its use would not infringe privately owned rights. Reference herein to any specific commercial product, process, or service by its trade name, trademark, manufacturer, or otherwise, does not necessarily constitute or imply its endorsement, recommendation, or favoring by the United States Government or any agency thereof, or The Regents of the University of California. The views and opinions of authors expressed herein do not necessarily state or reflect those of the United States Government or any agency thereof or The Regents of the University of California and shall not be used for advertising or product endorsement purposes.

Lawrence Berkeley Laboratory is an equal opportunity employer.

DISCLAIMER

This document was prepared as an account of work sponsored by the United States Government. While this document is believed to contain correct information, neither the United States Government nor any agency thereof, nor the Regents of the University of California, nor any of their employees, makes any warranty, express or implied, or assumes any legal responsibility for the accuracy, completeness, or usefulness of any information, apparatus, product, or process disclosed, or represents that its use would not infringe privately owned rights. Reference herein to any specific commercial product, process, or service by its trade name, trademark, manufacturer, or otherwise, does not necessarily constitute or imply its endorsement, recommendation, or favoring by the United States Government or any agency thereof, or the Regents of the University of California. The views and opinions of authors expressed herein do not necessarily state or reflect those of the United States Government or any agency thereof or the Regents of the University of California.

LBL-30571

THE EFFECT OF SURFACE RECONSTRUCTION ON THE CAPACITANCE OF Au(100) SURFACES

Philip N. Ross† and Alfred T. D'Agostino‡

†Materials Sciences Division
Lawrence Berkeley Laboratory
One Cyclotron Road
Berkeley, CA 94720

‡Department of Chemistry
University of South Florida
Tampa, FL 33620

This work was supported by the Director, Office of Energy Research, Office of Basic Energy Science, Materials Sciences Division of the U.S. Department of Energy under Contract Number DE-AC03-76SF00098.

LBL-30571

THE EFFECT OF SURFACE RECONSTRUCTION ON THE CAPACITANCE OF Au(100) SURFACES

Philip N. Ross† and Alfred T. D'Agostino‡

†Materials Sciences Division
Lawrence Berkeley Laboratory
One Cyclotron Road
Berkeley, CA 94720

ABSTRACT

The effect of reconstruction of the Au(100) surface on the double-layer capacity was measured using standard ac methods combined with UHV surface preparation and ex-situ structure analysis. The (5×20) reconstruction present on the UHV-prepared surface was found to be stable in dilute $HClO_4$ over a wide range of electrode potential. In dilute H_2SO_4, the (5×20) reconstruction was lifted at potentials near the pzc by specific adsorption of HSO_4^- even when the anion was present at very low concentrations, e.g. 10^{-5} M. In 0.01M $HClO_4$, the reconstruction was lifted only at potentials 0.2 V positive of the pzc, and was restored when the potential was made ca. 0.1 V negative of the pzc for the (1×1) surface, i.e. the $(5 \times 20) \rightleftarrows (1 \times 1)$ transformation was quasi-reversible in dilute $HClO_4$. Atomic scale roughness, e.g. steps, appeared to lower the stability of the (5×20) structure. The capacity curve for the (5×20) reconstructed surface was dramatically different from that of the (1×1) surface, with a negative shift in the pzc of ca. 0.2 V following the transformation $(5 \times 20) \rightarrow (1 \times 1)$, and a decrease in the capacitance of 20-25%, approximately equal to the change in atomic density of the surface. The vacuum work functions (Φ) of the emersed (5×20) and (1×1) surfaces were measured using photoemission spectroscopy, and found to be $5.30 \pm .05$, and $5.05 \pm .05$ eV, respectively, a $\Delta\Phi$ consistent with the relative values of the pzc's. Our results were consistent in every respect with the previous findings of Kolb and co-workers on the effect of reconstruction on the double-layer capacity of Au(100) surfaces.

‡ Present Address:

Department of Chemistry
University of South Florida
Tampa, FL 33620

INTRODUCTION

One of the most confounding complications in fundamental studies in electrochemistry using single crystals is that the equilibrium structure of the clean surface is not necessarily a regular termination of the bulk, i.e. it is reconstructed. Au is the most extreme example of this phenomenon, where all the low index surfaces, even the (111) surface, are reconstructed [1,2]. The clean surface of Au(100) has a now well-known reconstructed surface that was first characterized by Fedak and Gjostein as (5 × 20) [3,4]. The (100) faces of Ir, Pt and Au all exhibit reconstructed LEED patterns in UHV which have the nominal designation "(5 × 20)". In recent refined analysis by Van Hove et. al. [5], there are subtle differences in the diffraction patterns between these metals, and even between the patterns observed with the same metal. In the case of Au(100), Van Hove et. al. suggest the definitive reconstructed surface is c (26 × 28) not (5 × 20), but the basic real space structures are not very different, i.e. a hexagonal overlayer on a square sublattice [3,4]. Therefore, for our purposes here, and for convenience, we shall use the designation (5 × 20) in referring to the reconstructed surface of Au(100) throughout this paper.

The stability of the Au(100) - (5 × 20) surface in electrolyte has been studied extensively by Kolb and co-workers [6-9] using a combined UHV-electrochemical system and LEED analysis of emersed electrodes. They have also published capacitance curves [6-8] which show dramatic changes in the shape of these curves when the reconstruction is lifted, and reported a ca. - 0.2 V shift in the pzc between (100) - (5 × 20) and (100) - (1 × 1) surface. Kolb and Schneider [6,7] reported that the (5 × 20) reconstruction is stable in 0.01 M $HClO_4$ up to a potential ca. 0.2 V above the pzc, but in acids with specifically adsorbing anions (HSO_4^-, Cl^-) the (5 × 20) → (1 × 1) transformation is shifted negatively by 0.2 - 0.4 V, depending on the anion and the concentration. They concluded that specific adsorption of the anion, even in

perchloric acid, was the mechanism for lifting the reconstruction. They also reported that the (5×20) structure can be restored from a (1×1) by negative polarization, e.g. -0.5 V vs. the pzc. Recently, Ocko et. al. [10] reported an in-situ x-ray diffraction analysis of the structure of Au(100) surface in 0.01 M $HClO_4$ as a function of potential, results that were completely consistent with the ex-situ LEED results by Kolb and Schneider [6,7], including the potential induced $(1 \times 1) \rightarrow (5 \times 20)$ transformation. These studies provide very convincing evidence that the $(5 \times 20) \rightleftarrows (1 \times 1)$ transformations are quasi-reversible and occur in a potential region that is within ± 0.5 V of the pzc of either surface.

However, there are recent papers that dispute the existence of the (5×20) surface in electrolyte, including a paper from the present authors [11]. In a comment that was published [12] adjoining the paper by Kolb and Schneider [8], Hamelin disputed the electrochemical evidence for a $(1 \times 1) \rightarrow (5 \times 20)$ transformation, reporting capacity curves that varied only slightly with negative polarization. In a recent more extensive paper [13], Hamelin and co-workers present numerous capacity curves for Au(100) that show no sign of the $(5 \times 20) \rightleftarrows (1 \times 1)$ phenomenon, all the curves look like the curves attributed to a (1×1) structure by Kolb and Schneider. In our own previous work [11], we were unable to emerse a (5×20) structure from either 0.3 M HF or 0.01 M $HClO_4$ at any potential, and suggested that impurities from the electrolyte were stabilizing the (5×20) structure observed by Kolb and Schneider. We did not measure capacity curves, but the cyclic voltammetry curves did not show the distinct features Kolb and Schneider attributed to the $(5 \times 20) \rightarrow (1 \times 1)$ transformation.

In this paper, we report a re-examination of the $(5 \times 20) \rightleftarrows (1 \times 1)$ phenomena with an emphasis on the electrochemical evidence in terms of capacity curves. Shortly after the

publication of our paper in 1987 [11], we determined that our failure to observe the (5×20) surface on any emersed electrode was due to Cl adsorption on the emersed electrode during pump down and transfer to the UHV chamber [14]. Our failure to detect Cl contamination on our emersed electrodes was due to electron beam-stimulated desorption during Auger analysis [41]. The source of Cl was HCl/Cl_2 desorbing from the stainless steel walls of the transfer chamber during pump down following emersion. The chlorination of the walls was caused by repeated exposure to HF vapor containing a partial pressure of HCl of at least 10^{-4} torr. Rebuilding the transfer chamber with new specially polished components eliminated the HCl/Cl_2 outgassing during pump down and transfer, and we were able to observe the (5×20) LEED pattern from emersed Au(100) electrodes [14]. We report here our new findings on the stability of the (5×20) reconstruction in electrolyte using ex-situ LEED and the effect of the $(5 \times 20) \rightleftarrows (1 \times 1)$ transformation on capacitance. The results are in complete agreement with the reports by Kolb and co-workers, and we report new results which show that atomic scale roughness (e.g. steps) impedes the potential induced $(1 \times 1) \rightarrow (5 \times 20)$ transformation, offering a possible explanation for the capacitance curves reported by Hamelin and co-workers.

EXPERIMENTAL

The UHV-electrochemistry system has been described in detail previously [15]. The experimental procedures were exactly the same as in our previous paper [11], with the difference being that the transfer chamber was rebuilt to remove the HCl/Cl_2 contamination problem discussed above. The UHV system had the additional capability of photoelectron spectroscopy, being equipped with a double-pass CMA (PHI Model 15-255) and both x-ray (PHI Model) and VUV (PHI Model 1500) sources. Surface cleanliness was monitored by use of x-ray photoelectron spectroscopy (XPS) rather than AES as in our previous paper [11]

in order to avoid stimulated desorption of Cl. The detection limit for Cl and C on Au by electron spectroscopy is of the order of a few percent of a monolayer [42]. Work functions of surfaces in vacuum were measured from the width of the photoemission band using He I ($h\nu$ = 21.22 eV) photons with analyzer operated in the constant pass energy mode with a pass energy of 25 eV. The precision of our work function measurements was estimated to be $\pm$0.05 eV by repeating the measurements with different crystals of the same orientation. The absolute accuracy of work functions determined using photoemission spectroscopy in modern UHV systems is estimated to be $\pm$ 0.1 eV [43]. Capacitance curves were recorded potentiodynamically using a potentiostat (PAR Model 173) and a two-phase lock-in amplifier (Ortec Model 9502). A 5 mV oscillation at 20 Hz was superimposed on a 5 mV/s voltage sweep and the capacitance calculated from the real and imaginary parts of the current [16]. The reference electrode used in this apparatus is α-PdH. However, all potentials in this paper are reported versus a reversible hydrogen (1 atm.) electrode in the same electrolyte (nhe).

RESULTS

Actual LEED patterns will not be shown here, as we observed only two different patterns, either the (5 × 20) or the (1 × 1), and both patterns have been shown several times by both Kolb and co-workers [6,9] and by ourselves [11]. We will simply report which of the two patterns were observed under various conditions of emersion.

A sequence of capacity curves in 0.01 M $HClO_4$ for a Au(100) surface exhibiting a (5 × 20) LEED pattern in UHV is shown in Figures 1-4. The crystal was brought into contact with electrolyte under potentiostatic control at 0.1 V. The first sweep was positive to 0.8 V, then the sweep was reversed back to 0.1 V. As we shall discuss in greater detail below this curve looks qualitatively like the curve reported by several groups [9,17,18] for Au(111), but the "flat-bottom" minimum in the capacity at 0.45 - 0.6 V is not seen on Au(111). The curve

in Figure 1 was quite stable to repeated cycling between these potentials. Emersion of the electrode at 0.8 V produced the (5 × 20) LEED pattern. Figure 2 shows the capacity curves for the second sweep after reversal at 0.1 V, with the positive limit raised to 1.0 V. Above 0.8 V, the capacity dropped quite sharply from ca. 60 $\mu F/cm^2$ to about 35 $\mu F/cm^2$. On reversing the sweep at 1.0 V, the curve for the negative sweep is completely different from that on the positive sweep, and qualitatively resembles that reported by Hamelin [12,13] for Au(100). Emersion of the electrode at 1.0 V produced the (1 × 1) LEED pattern.

Figure 3 shows the curves for the third cycle in this sequence with the same potential limits as in Figure 2. These curves were relatively unchanged in 2-3 subsequent cycles between these potential limits. Figure 4 shows the curves when the negative limit was reduced to 0.3 V. Emersion of the electrode at <u>either</u> potential limit produced a (1 × 1) LEED pattern.

The capacity curves in Figure 3 are very similar to the capacity curves of Kolb and Schneider [Fig. 1 in ref. 7] under very similar conditions, and our interpretation of them is the same. The curve on the positive sweep, with a pzc at 0.6 V, is characteristic of a (100) - (5 × 20) surface; the curve on the negative sweep, with a pzc at 0.4 V, is characteristic of the (100) - (1 × 1) surface. The transformation (5 × 20) → (1 × 1) occurs at 0.8 - 0.9 V, the transformation (1 × 1) → (5 × 20) occurs at 0.1 - 0.2 V. Under these conditions of cycling, neither transformation is complete, the curves have some elements of the curve of both surfaces. We agree with Kolb and Schneider that the incomplete transformation produces patches of each structure within the other.

The sharp drop in capacitance above 0.8 V is the electrochemical signature of the (5 × 20) → (1 × 1) structural transformation. This can be seen by comparing the capacity curve on the positive sweep for the (5 × 20) surface with the curve for Au(111) - (1 × 1) which is the structural analog to the top layer of the (5 × 20) surface. The comparison is shown in Figure

5. The curve labelled Au(111) - (1 × 1) was recorded on the second positive sweep after the first sweep lifted the (1 × 23) reconstruction on the UHV prepared surface [9]. For the (111) electrode, the capacity at 0.9 - 1.0 V is about 50 $\mu F/cm^2$, whereas the capacity for the (100) electrode is the same potential region (which has the (1 × 1) structure) is about 35 $\mu F/cm^2$. This difference in capacity corresponds approximately to the difference in atomic density between (111) or (100) - (5 × 20) and (100) - (1 × 1) surface structures [3,4], i.e. 22%.

Kolb and Schneider also reported capacity curves in 0.01 N H_2SO_4. Our comparable curve for Au(100) is shown in Figure 6. As in Figure 1, the (100) crystal with the (5 × 20) LEED pattern in UHV was contacted with electrolyte while potentiostatted at 0.1 V, the first capacity curve recorded on a positive sweep to a limit of 0.8 V, then the first negative sweep curve recorded. The negative sweep capacity curve has a completely different shape to the positive sweep curve. These two curves are almost quantitatively the same as the curves reported by Kolb and Schneider [Fig. 3 of ref. 7]. We agree with those authors that the dramatic hysteresis in Fig. 6 reflects the (5 × 20) → (1 × 1) transformation in the potential region above 0.7 V, about 0.2 V lower than the transformation potential in 0.01 N $HClO_4$. This lowering of the transformation potential is due to specific adsorption of HSO_4^-.

One can appreciate the effect of specific adsorption of HSO_4^- on the capacity curves by looking at a wider range of potential than in Fig. 6, and by comparison of the capacity curves from a (100) crystal and a (111) crystal. Figure 7 shows the capacity curves in 0.01 M $HClO_4$ and in 0.01 N H_2SO_4 for a Au(111) electrode recorded on the second positive sweep to 1.2 V, and thus represent the capacity of the (111) - (1 × 1) surface throughout the potential range of 0.2 - 1.2 V. The much higher (5-fold) capacitance in H_2SO_4 in this potential range is clearly indicative of an adsorption pseudo-capacitance, specific adsorption of HSO_4^- with charge transfer. The HSO_4^- adsorption pseudo-capacitance has its onset at about 0.5 V, just

negative of the pzc in 0.01 M $HClO_4$, although there are differences in capacitance at lower potentials that suggest there is some adsorption of HSO_4^- even at 0.1 - 0.5 V. The shaded region in the figure indicates the total charge that can be attributed to HSO_4^- adsorption pseudo-capacity, which in this case was 32 $\mu C/cm^2$. The concentration dependance of this charge is shown in Figure 8. In 0.01 N H_2SO_4, there is a sharp local minimum ($dC/dV = 0$) at about 0.6 V, which is close to the potential as the more classically shaped capacitive minimum in 0.01 M $HClO_4$ (Figure 4). This minimum at 0.6 V disappeared at H_2SO_4 concentrations above 0.05 N, became more pronounced (and broader) at concentrations below 0.01 N, and shifted negatively in potential. These concentration effects are characteristic of a diffuse layer minimum at the pzc in the <u>absence</u> of specific adsorption [13], a puzzling result for this electrolyte.

Figure 9 shows the capacity curves for Au(100) - (5 × 20) superimposed on the curves for Au(111) - (1 × 1) with the potential range of the positive sweep on the (100) crystal extended to 1.2 V. As was the case in $HClO_4$, the capacitance for Au(100) - (5 × 20) followed that for the Au(111) - (1 × 1) surface up to a potential that is 0.1 - 0.2 V positive of the pzc, above which there was a significant difference in capacitance due to the (5 × 20) → (1 × 1) transformation. However, in H_2SO_4, because of specific adsorption of HSO_4^-, this difference in capacitance is not the small factor (25% higher capacitance on (111) - (1 × 1) than (100) - (1 × 1)) that it is in $HClO_4$, representing just the difference in atomic (electron) density. Rather it is a factor of 3 - 5 times higher capacity on Au(111) - (1 × 1) than on Au(100) - (1 × 1) in this potential range. This surprising difference in HSO_4^- adsorption pseudo-capacitance between Au(111) and Au(100) was observed previously by Angerstein - Kozlowska et. al. [19]. Applying their reasoning to the present results, it appears that following the (5 × 20) → (1 × 1) transition induced by a critical level of HSO_4^- adsorption, HSO_4^- adsorption continues to

increase with increasing potential on the (1 × 1) surface, but the character of the adsorption is different (little or no charge transfer) due to the difference in surface symmetry. The critical level of HSO_4^- that lifts the reconstruction, expressed in terms of charge, can be estimated by integrating the capacity curve (positive sweep) from 0.5 V to 0.7 V, which yields 8 $\mu C/cm^2$.

The reversibility of the $(5 \times 20) \rightleftarrows (1 \times 1)$ transformation, especially the ability to reform the (5 × 20) from the (1 × 1) by negative polarization, was found to depend on the pretreatment of the electrode surface. For example, the reversible behavior shown in Figure 4 could not be observed when the cycling in this region of potential continued. Kolb [20] has attributed this to progressive roughening of the surface each time the reconstruction is lifted, since the 22% change in atomic density causes islands of the "extra" Au atoms to be formed on the surface. We examined this concept by re-structuring the surface in UHV by evaporation of 2 ML of Au onto the Au(100) - (5 × 20) surface and partially annealing at 300°C i.e. auto-epitaxy of Au on Au. According to the STM study by Lang et. al. [40], epitaxial growth of Au on Au(111) proceeds via nucleation of monatomically high clusters ("islands"), and we expected a similar growth mechanism for Au(100). The LEED pattern for our Au/Au(100) structure was consistent with a similar epitaxial island structure, sharp (1 × 1) fundamental spots with "streaks" rather than spots for 1/5 th and 1/20 th order spots. The capacitance curves for this surface in 0.01 M $HClO_4$ are shown in Figure 10. The first positive sweep shows a mixed character of (1 × 1) and (5 × 20), but after the (5 × 20) → (1 × 1) transformation was lifted at 0.9 V, the next positive sweep showed only (1 × 1) character. This was the only surface in this study which produced the classically shaped C(V) curve with a pzc at 0.4 V <u>on the positive sweep</u>, i.e. after slow potential scanning thru 0.1 V. Holding the potential at 0.1

V for 100 sec did not change the shape of the C(V) curve significantly. This surface was the only Au(100) surface in our study that produced C(V) curves similar to those reported by Hamelin [12,13] for Au(100).

Work functions were measured in UHV for the clean annealed (100) - (5 × 20) surface, and for the (5 × 20) and (1 × 1) surfaces emersed from 0.01 M $HClO_4$ at their respective pzc's. Work functions were not measured for any surfaces emersed from 0.01 N H_2SO_4 since XPS spectra indicated the presence of sulfate on the surface and the LEED patterns had faint (100) - p (2 × 2) spots attributed to a layer of H_2SO_4 [21]. Electrodes emersed from 0.01 M $HClO_4$ appeared clean by XPS. The work function of the clean annealed (100) - (5 × 20) was 5.35 ± 0.05 eV, while that of the (5 × 20) emersed was 5.45 eV, and that of the (1 × 1) emersed was 5.20 eV. For comparison, the work function of the clean annealed Au(111) - (1 × 23) surface was 5.40 eV, while that of emersed Au(111) electrodes (there was no measurable difference in Φ between emersed (1 × 23) and (1 × 1) surfaces) was 5.50 eV. LeCoeur et. al. [18] reported a vacuum work function of 5.30 ± .05 eV for clean annealed Au(111) using the same photoemission method as here. The approximately 0.1 eV higher work function for emersed Au(100) - (5 × 20) and (111) - (1 × 23) surfaces versus their clean annealed counterparts is thought to be due to the presence of trace amounts of impurity anions, e.g. HSO_4^- and Cl^- [22], remaining on the surface after emersion. The work function measurements are summarized in Table 1.

DISCUSSION

To our knowledge, this is the first report of the work functions for emersed Au(100) and (111) electrodes. The difference in work function between the emersed (100) - (5 × 20) and (100) - (1 × 1) surfaces was + 0.25 (± 0.1) eV, which is very close to the observed difference in the pzc's of those surfaces in 0.01 M $HClO_4$, 0.2 (± 0.05) V. The potential of zero charge

for a metal surface is directly related to the vacuum work function [23]. One of the expressions frequently used for this relation for a metal M having the crystal plane (hkl) at the metal-solution interface is,

$$E^{(hkl)}_{\sigma=0} = \Phi^{(hkl)}/e - [\delta\chi^{(hkl)} + g^{S}_{hkl}(dip)]_{\sigma=0} + K \qquad (1)$$

where $[\delta\chi^{(hkl)} + g^{s}_{hkl}(dip)]\sigma = 0$ represents the potential drop at the M(hkl) - solution interface, arising from a change $\delta\chi$ in the electronic structure of the metal due to the contact with water and the dipole contribution $g^{S}_{hkl}(dip)$ for water molecules at the surface, and K is a constant due to the potential drop at the reference electrode - solution interface. Lecoeur et.al. [24] have analyzed the variation of the $\delta\chi$ and g^{s}_{m} terms for different Au(hkl) faces, and concluded that

$$[\delta\chi^{(hkl)} + g^{s}_{hkl}(dip)]_{\sigma=0} - [\delta\chi^{(h'k'l')} + g^{s}_{h'k'l'}(dip)]_{\sigma=0} < 0.1\,eV \qquad (2)$$

so that to a first approximation we would expect

$$E^{(hkl)}_{\sigma=0} - E^{(h'k'l')}_{\sigma=0} \doteq [\Phi(hkl) - \Phi(h'k'l')]/e \qquad (3)$$

As can be seen from the results in Table 1, the pzc's and Φ's we found were clearly consistent with this expectation.

With respect to the capacity curves, and the effect of the $(5\times20)\rightleftarrows(1\times1)$ transformations on capacitance, there is not a great deal new to say, Kolb and Schneider have already described the effect extensively, and our results are in complete agreement with theirs. However, there is still considerable uncertainty about the energetics of these transformations, both the thermodynamic driving force and the source of energy to move the Au atoms around during these structural transformations <u>at room temperature</u>. Theoretical calculations [25] have shown that the difference in surface energy

between the clean (5×20) structure and the (1×1) structure is about 0.1 eV/atom (≈ 220 dynes/cm), which is small relative to chemisorption energies, which are typically 1 - 5 eV/atom, or to the activation energy for surface self-diffusion, which is typically about 1 eV [26]. Tomanek and Bennemann [25] have presented a very useable theoretical model for showing how chemisorption can either lift the reconstruction, e.g. CO adsorption on Pt(100) induces $(5 \times 20) \rightarrow (1 \times 1)$, or induce the reconstruction, e.g. H_2 adsorption on Pd(110) induces $(1 \times 1) \rightarrow (1 \times 2)$, since the total surface energy is dominated by the contribution of the adsorption energy and the dependence of the adsorption energy on surface structure. Because the adsorption energy is typically so much larger than the difference in surface energy between the reconstructed and unreconstructed surfaces, the coverage by the adsorbate necessary to produce the surface transformation is typically quite small, especially for the alkali metal induced reconstructions, e.g. 0.05 ML of Cs on Pd(110) [27]. A similar argument can be applied to the activation energy, i.e. the source of thermal energy necessary to overcome the activation barrier for surface self-diffusion comes from the (exothermic) heat of adsorption.

The same kind of total surface energy calculations can be made for the electrochemical interface. The theory of electrocapillarity relates the change in interfacial tension to the electrode potential [28]. Originally developed for mercury, a liquid metal surface whose interfacial tension could be measured directly, the same concepts and equations can be applied to solid metals [29]. Lin and Beck [30] used a sensitive extensometer to measure the interfacial tension curve for polycrystalline gold. We can use their curves, and apply them to examine the thermodynamic driving force for the $(5 \times 20) \rightleftarrows (1 \times 1)$ transformation. To make those calculations, we make the following assumptions: the difference in interfacial tension at the

pzc between the (5×20) and (1×1) surfaces is 220 dynes/cm,‡ the value calculated by Tomanek and Bennemann [25] for the clean metal surfaces; in the absence of anion adsorption the γ (V) curve is given by the Helmholtz - Perrin equation.

$$(\gamma - \gamma_{max}) = \frac{C}{2} (E - E_{\sigma=0})^2 \tag{4}$$

where C is the double-layer capacity at very negative potentials, e.g. 17 μ F/cm^2. Figure 11 shows the two electrocapillary curves calculated for the (5×20) and (1×1) surfaces with these assumptions. It is easily seen that in the absence of anion adsorption, the change in interfacial tension produced by potential is too small to compensate for the lower surface energy of the (5×20) surface. If we use the experimental values for the effect of Cl^- adsorption on the surface energy of polycrystalline gold in 0.1 N KCl [30], assuming that Cl^- adsorption has the same effect on γ as a function of $(E - E_{\sigma=0})$ on both surfaces, then we see via the dashed curves that the γ (V) curve for (1×1) surface now crosses over the curve for the (5×20) surface, thus driving the transformation $(5 \times 20) \rightarrow (1 \times 1)$. The cross-over potential depends on the <u>relative</u> lowering of the interfacial tension by anion adsorption. When the anion has the same adsorption energy on both surfaces, then the curves constructed from Lin and Beck's data show a cross-over at about 0.9 V. If the anion adsorption were significantly stronger on the (1×1) surface, as is usually the case in the adsorption of neutral molecules on metal surfaces, then the cross-over potential can be much closer to the pzc, as shown by the hypothetical curve for (1×1) in Figure 11. These considerations provide a semi-quantitative theoretical basis for the intuitive concept that specific anion adsorption is the process that drives the $(5 \times 20) \rightarrow (1 \times 1)$ transformation, as suggested earlier by Kolb and Schneider [9].

‡ 1 dyne/cm = 10^{-5} N/cm

However, while the interfacial tension curves of Lin and Beck [30] for gold in Cl^- and HSO_4^- electrolytes indicate that adsorption of these anions can lower the total surface energy by the amount required to drive the transformation, there is no such data, even for mercury, that indicates that ClO_4^- anion adsorption can do the same. In this regard, there is a concern about adsorption of impurity anions, e.g. Cl^- and HSO_4^-, present in even the purest $HClO_4$ [22]. The amount of Cl^- on HSO_4^- adsorption necessary to drive the reconstruction is quite small. This can be seen either by integration of the experimental capacity curves from the pzc to the transition potential, since by definition $C = dq/dV$ or by differentiation of the semi-theoretical interfacial tension curves, (Fig. 11). Integration of the capacity curves in either H_2SO_4 or $HClO_4$ gives approximately the same charge for the transformation, $8\,\mu C/cm^2$. Differentiation of the electrocapillary curves at the cross-over point gives $5\text{-}10\,\mu C/cm^2$. These coverages indicate very small quantities of adsorption if we consider a monolayer of charge to be of the order of $100\text{-}200\,\mu C/cm^2$, i.e. one anion to every ten or twenty gold atoms. The bulk concentration of anions in equilibrium with such a small surface concentration can in turn be quite small. Extrapolation of the HSO_4^- charge observed on Au(111), reported in Figure 8, indicates a bulk concentration of ca. 2×10^{-5} M H_2SO_4 would result in adsorption of HSO_4^- to the required level of coverage. Nonetheless, if one uses high purity reagents and careful experimental procedures, this level of impurity is not likely to occur in 0.01 N $HClO_4$, but is certainly a possible level [22] in lN $HClO_4$, and may be a factor in the $HClO_4$ concentration effect reported by Kolb and Schneider [8].

If impurity adsorption in 0.01 N $HClO_4$ is not a likely possibility, and if ClO_4^- adsorption is very weak, what then is the driving force for the $(5 \times 20) \rightarrow (1 \times 1)$ transformation. Kolb and Schneider [7] have suggested "OH" adsorption, a precursor state to positive oxide formation. We offer another possible explanation, and one which is certainly less conventional. It is

based on the consideration of surface electron density, and a contribution of surface electron density to the surface energy that is unique to solid metal surfaces (vs. liquid metals like Hg). The origin of the concept is the known effect of alkali metals in causing a reconstruction of certain fcc (110) metal surfaces that are not normally reconstructed in vacuum, e.g. the (1×2) missing-row reconstruction of Au(110) by less than 0.1 monolayer of K [31], and in stabilizing the (5×20) reconstruction of Pt(100) even in the presence of molecular adsorbates that lift the reconstruction [32]. The effects of alkali metals in these phenomena cannot be explained by the simple chemisorption model, such as that of Tomanek and Bennemann [25]. Ho and co-workers [33,34] have proposed a charge density model to explain the reconstruction of both Ag(110) and Au(110) by K. They have also shown that a simple external electric field can induce the (1×2) reconstruction on Ag(110) [33]. The surface energy in the presence of a field decreases as the number of induced surface electrons increases. The negatively charged surface undergoes a structural transformation from (1×1) to (1×2) as the number of induced electrons reaches a value of $\cong 0.05$ e/atom or 6.5 $\mu C/cm^2$, which corresponds to a field strength of $\cong 10^7$ V/cm. These magnitudes of surface charge and field strength are exactly what one would expect for a metal like Ag or Au at a potential $\cong 0.2 - 0.4$ V negative of the pzc in <u>non-adsorbing</u> electrolyte. While it is not stated specifically in their paper, one may reasonably infer that with positively charged surface the opposite would occur, that the (1×1) structure has a lower surface energy than the (1×2). Ku and Ho [33] refer to this effect of surface electron density as "s,p compression". We suggest this same principle may account for the potential induced $(5 \times 20) \rightleftarrows (1 \times 1)$ transformations in electrolyte where neither ion is specifically adsorbed, such as in $HClO_4$.

Our experiment with an intentionally "roughened" Au(100) crystal appears to offer a reconciliation between the capacitance curves for Au(100) of Hamelin and co-workers and Kolb and co-workers. For example, the most recent C - V curves of Hamelin and co-workers [13] showed no signs of the dramatic hysteresis between the positive and negative sweeps that we, and Kolb and Schneider, attribute to the $(5 \times 20) \rightleftarrows (1 \times 1)$ phenomena. The explanation we offer for this is that the (100) surfaces of Hamelin and co-workers had a high step density, due either to "roughening" from potential cycling or to the method of sample preparation. The role of steps in suppressing reconstruction can be rationalized in two ways, a simple geometric argument, and an electrostatic argument. The unit cell of the (5×20) structure is very large, approximately 15×60 Å. If the step density in the (1×1) structure is higher than 1.7×10^6 cm^{-1} in both the [010] and [001] directions of the surface, then there are not enough atoms in same surface domain to form a unit cell, destabilizing the (5×20) structure. There is also an electrostatic rationale. The (5×20) overlayer has a higher electron density than the underlying bulk lattice, creating a surface dipole with the negative end up. On the other hand, the abrupt discontinuity at an atomic step creates a local dipole at the step [35] with the positive end up. Thus, the steps have to be eliminated to form the intrinsically negatively charged (5×20) overlayer.

Finally, we feel it is important to comment on the relation of the surface reconstruction on the stability of high Miller index Au single crystal surfaces. High Miller index surfaces are of interest to surface scientists who want to examine the role of step-like surface imperfections and want to control the step density and step geometry in regular way [36]. However, the use of Miller index surfaces to accomplish this regular variation depends critically on the formation of the ideal bulk termination structure, a step-terrace configuration with atomically flat terraces of known width connected by monatomically high steps [37]. The surface structure

on high Miller index crystals of Pt were studied extensively by Blakely and Somorjai [38]. It is clear that the thermodynamic driving force for reconstruction causes faceting to occur on crystals cut a few degrees from the [100] and [110] poles, e.g. the Pt (511) crystal ideally would form the 3(100) - (111) step-terrace structure, but it facets to form reconstructed (5 × 20) facets connected by multiatomic steps [38]. There are no studies known to us of the structure of a Au(hkl) surface with h, k, or l > 3. There is one study of a Au surface with h, k, l > 2, the Au(311) surface by Sotto and Boulliard [39]. This surface was found to form a complex reconstruction in UHV, and did not form the ideal step-terrace structure 2(100) - (111). In the absence of sufficient surface structure analysis, one might expect that high Miller index Au crystals will behave like their Pt counterparts with respect to the effect of reconstruction on the ideal step-terrace structure, but given the fact that the clean annealed surfaces of all three low index faces of Au are reconstructed, even the [m(111) × (100)] and [m(111) × (111)] structures expected to form on Au crystals cut a few degrees from the [111] pole may not in fact be formed. The lifting of the (5 × 20) reconstruction on (100) domains in electrolyte does not mitigate this concern, since faceting would already have occurred during thermal annealing in surface pre-treatment. Until a great deal more is learned about the surface structure of the high Miller index surfaces of Au, one cannot reasonably assume that high Miller index faces of Au can be used to explore the role of monatomic steps in electrode processes.

ACKNOWLEDGMENT

The authors acknowledge invaluable assistance from Prof. D. Sherson, Case Western Reserve University, with the techniques for capacitance measurement. The authors are also grateful to Prof. J. Lipkowski, University of Guelph, for informative discussions on the classical theory of electrocapillarity and for directing us to the seminal papers by Beck and Mohilner. This work was supported by the Director, Office of Energy Research, Office of Basic Energy Science, Materials Sciences Division of the U.S. Department of Energy under Contract Number DE-AC03-76SF00098.

Table 1

Relationship Between Work Function and Potential of Zero Charge for a Variety of Au Single Crystal Surfaces		
Surface	$E_{\sigma=0}$ **(V/nhe)**	Φ **(eV)**
Au(111) - (1 × 23)	0.65 ± 0.02	5.50 ± .05[1]
Au(111) - (1 × 1)	0.60 ± 0.02	5.50 ± .05[1]
Au(100) - (5 × 20)	0.55 ± 0.05	5.45 ± .05[1]
Au(100) - (1 × 1)	0.40 ± 0.02	5.20 ± .05[1]
Au(100) - (5 × 20)	-	5.35 ± .05[2]
Au(111) - (1 × 23)	-	5.40 ± .05[2]

1 Values for emersed surfaces

2 Values for the clean annealed surfaces

REFERENCES

1. D.M. Zehner and J.F. Wendelken, in: Proc. 7th Intern. Vacuum Congr. and 3rd Intern. Conf. on Solid Surfaces, Vienna, 1977, p. 517; Surface Sci. 71 (1978) 178.

2. V. Horten, A. Lahee, J. Toennies and Ch. Woell, Phys. Rev. Letters 54 (1985) 2619.

3. D. Fedak and N. Gjostein, Phys. Rev. Letters 16 (1966) 171.

4. D. Fedak and N. Gjostein, Surface Sci. 8 (1967) 77.

5. M.A. Van Hove, R.J. Koestner, P.C. Stair, J.P. Biberian, L.I. Kesmodel, I. Bartos and G.A. Somorjai, Surface Sci. 103 (1981) 189.

6. D. Kolb, G. Lehmpfuhl, and M. Zei, J. Electroannal. Chem. 179 (1984) 289.

7. D. Kolb and J. Schneider, Surf. Sci. 162 (1985) 764.

8. D. Kolb and J. Schneider, Electrochim. Acta, 31 (1986) 929.

9. M. Zei, G. Lehmpfuhl and D. Kolb, Surf. Sci. 221 (1989) 23.

10. B. Ocko, J. Wang, A. Davenport and H. Isaacs, Phys. Rev. Lett. 65 (1990) 1466.

11. A. D'Agostino and P. Ross, Surf. Sci. 185 (1987) 88.

12. A. Hamelin, Electrochim. Acta, 31 (1986) 1937.

13. F. Silva, M. Sottomayor, A. Hamelin and L. Stoicoviciu, J. Electroanal. Chem. 295 (1990) 301; for a review of previous work cf. A. Hamelin in "Modern Aspects of Electrochemistry", Vol. 16, B. Conway, R. White and J. Bockris, eds. (Plenum, New York, 1985) pp. 1-98.

14. P. Ross, Extended Abstracts, Volume 88-1, The Electrochemical Society, 1988, pp. 742-743.

15. P. Ross, and F. Wagner in: Advances in Electrochemistry and Electrochemical Engineering, Vol. 13, H. Gericher and C. Tobias eds. (Wiley, New York, 1984) p69ff.

16. W. Fawcett and R. Loutfy, J. Electroanal. Chem. 39 (1972) 185.

17. A. Hamelin, J. Electroanal. Chem. 210 (1986) 303.

18. J. Lecoeur, J. Bellier and C. Koehler, Electrochem. Acta, 36 (1990) 1383.

19. H. Angerstein-Kozlowska, B. Conway, A. Hamelin and L. Stoicoviciu, Electrochim. Acta, 31 (1986) 1051.

20. D.M. Kolb, personal communication, 1988.

21. M. Zei and D. Weick, Surf. Sci. 208 (1989) 425.

22. B. Cahan, H. Villullas and E. Yeager, J. Electroanal. Chem. 306 (1991) 213.

23. S. Trasatti, J. Electroanal. Chem. 33 (1971) 351.

24. J. Leceour, J. Andro and R. Parsons, Surf. Sci. 114 (1982) 320.

25. D. Tomanek and Bennemann, Surf. Sci. 163 (1985) 503.

26. G. Ehrlich in "Chemistry and Physics of Solid Surfaces V", R. Vanselow and R. Howe eds. (Springer Verlag, 1984), pp. 283-296.

27. C. Barnes, M. Ding, M. Lindroos, R. Diehl and D. King, Surf. Sci. 162 (1985) 59.

28. For a review, cf. D.M. Mohilner in "Electroanalytical Chemistry", Vol. 1, A.J. Bard, ed., Marcel Dekker, New York, 1966, pp. 241-409.

29. D. Mohilner and T. Beck, J. Phys. Chem. 83 (1979) 1160.

30. K. Lin and T. Beck, J. Electrochem. Soc. 123 (1976) 1145.

31. R. Behm, D. Flynn, K. Jamison G. Ertl and P. Thiel, Phys. Rev. B 36 (1987) 9267.

32. E. Garfunkel and G. Somorjai, Surf. Sci. 115 (1982) 441.

33. C. Fu and K.-M. Ho, Phys. Rev. Lett. 63 (1989) 1617.

34. K.-M. Ho, C. Chan and K. Bohnen, Phys. Rev. B, 40 (1989) 9978.

35. K. Besocke, B. Krahl-Urban and M. Wagner, Surf. Sci. 68 (1977) 39.

36. G. Somorjai, "Chemistry in Two Dimensions", Cornell University Press, Ithaca, 1981, pp. 156-168.

37. R. Joyner, B. Lang and G. Somorjai, Surf. Sci. 30 (1972) 440.

38. D. Blakely and G. Somorjai, Surf. Sci. 65 (1977) 419.

39. M. Sotto and J. Boulliard, Surf. Sci. 214 (1989) 97.

40. C. Lang, M. Dovek, J. Nogami and C. Quate, Surf. Sci. 224 (1989) L947.

41. E. Struve, R. Borup and D. Sauer, Proc. Symp. Appl. Surf. Analysis Methods to Environmental/Materials Interact., The Electrochemical Society, Pennington, NJ, 1991 (in press).

42. T. Carlson, "Photoelectron and Auger Spectroscopy", Plenum Press, New York and London, 1975, p. 323.

43. H. Michaelson, J. Appl. Phys. 48 (1977) 4729.

FIGURE CAPTIONS

Figure 1. Capacitance curves for a Au(100)-(5×20) reconstructed surface transferred from UHV and contacted with 0.01 N $HClO_4$ at 0.1 V. Emersion of the sample at 0.8 V and transfer to UHV produced a (5×20) LEED pattern.

Figure 2. Capacitance curves for the same sample as in Fig. 1 on the second positive sweep from 0.1 V, with the positive limit extended to 1.0 V. Emersion of the sample at 1.0 V and transfer to UHV produced at (100) - (1×1) LEED pattern.

Figure 3. Capacitance curves for the same sample as in Figs. 1 & 2 on the third consecutive sweep. Emersion of the sample at the potential limits shown produced in UHV the LEED patterns indicated in the figure.

Figure 4. Capacitance curves for same sample as in Figs. 1-3 with negative potential limit reduced to 0.25 V. Emersion of the sample at the potential limits shown produced in UHV the LEED patterns indicated in the figure.

Figure 5. Comparison of capacitance curves in 0.01 N $HClO_4$ on the positive sweep for a Au(100) - (5×20) surface, first sweep after transfer from UHV, and a Au(111) surface on second sweep after transfer from UHV and an positive sweep to 1.2 V to lift the (1×23) reconstruction [8]

Figure 6. Capacitance curves for a Au(100) - (5×20) reconstructed surface transferred from UHV and contacted with 0.01 N H_2SO_4.

Figure 7. Comparison of capacitance curves for a Au(111) surface in 0.01 N $HClO_4$ and 0.01 N H_2SO_4, second positive sweeps. Shaded area indicated indicates charge due to adsorption of HSO_4^- anion.

Figure 8. Concentration dependance of the charge in shaded region of Fig. 8 for Au(111).

Figure 9. Same experiment as in Figure 5 with a higher positive limit. For comparison, the curve for a Au(111) surface on the second potential scan in the same electrolyte is shown.

Figure 10. Capacitance curves in 0.01 N $HClO_4$ for a Au(100) surface "roughened" in UHV by vapor deposition of Au in (see text).

Figure 11. Theoretical electrocapillary curves for Au(100) - (1×1) and (5×20) without anion adsorption (——) and with two different types anion adsorption, (– –) same adsorption energy on both surfaces, (– · –) preferential adsorption on the (1×1) surface.

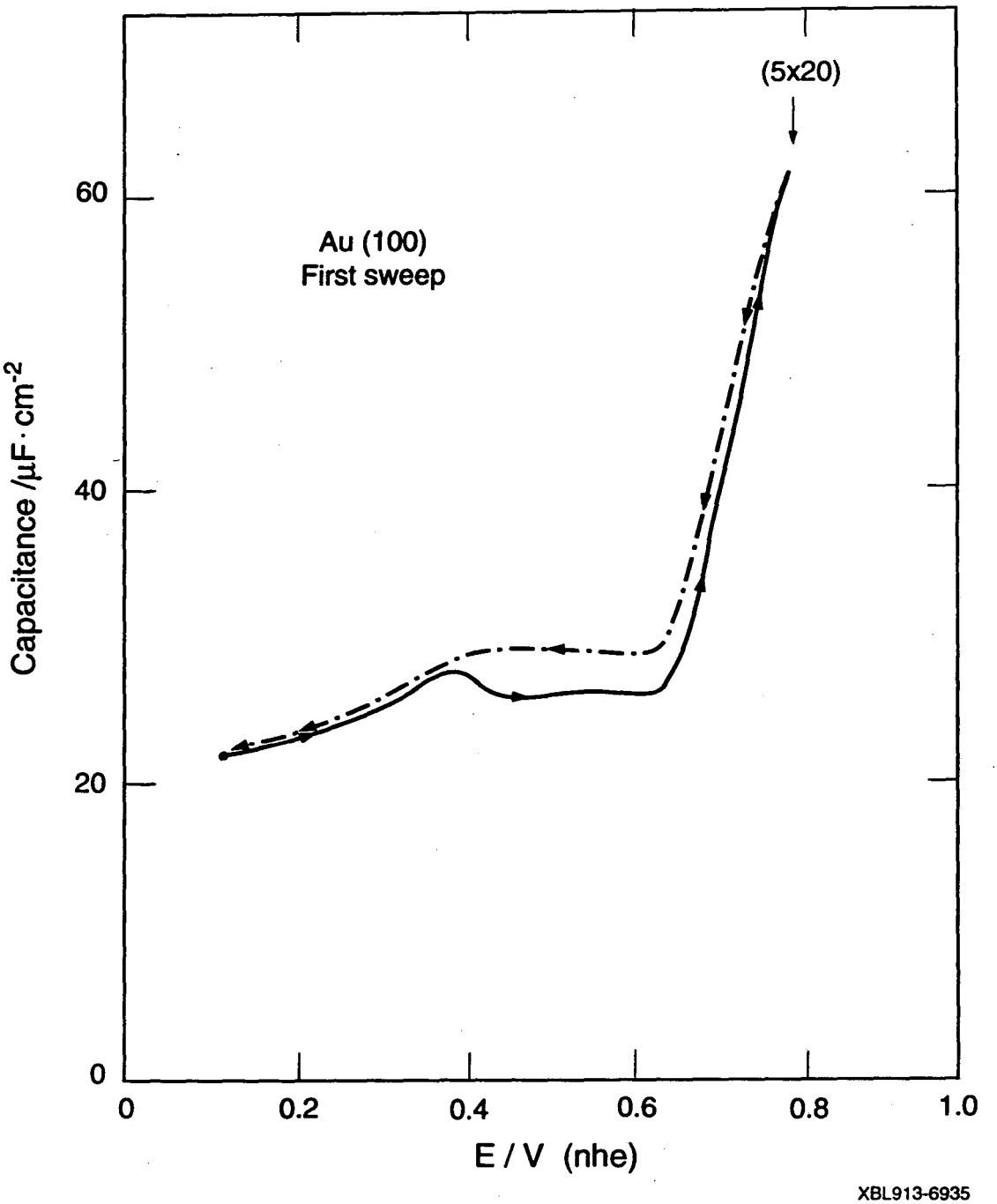
(5x20)
Au (100)
First sweep
Capacitance /μF · cm-2
60
40
20
0
0
0.2
0.4
0.6
0.8
1.0
E / V (nhe)
XBL913-6935

Figure 1

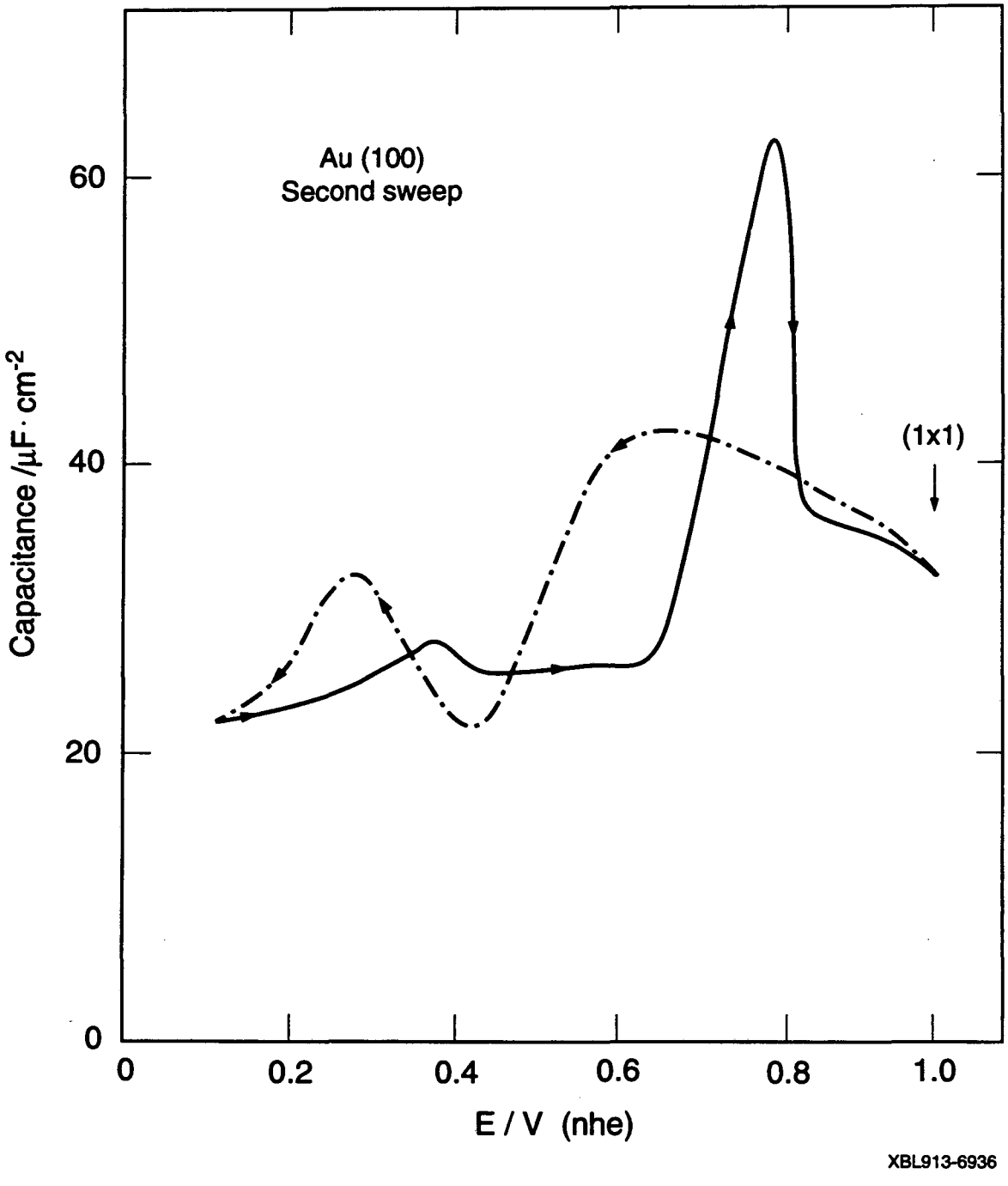
Au (100)
Second sweep
(1x1)
Capacitance /μF · cm-2
60
40
20
0
0
0.2
0.4
0.6
0.8
1.0
E / V (nhe)
XBL913-6936

Figure 2

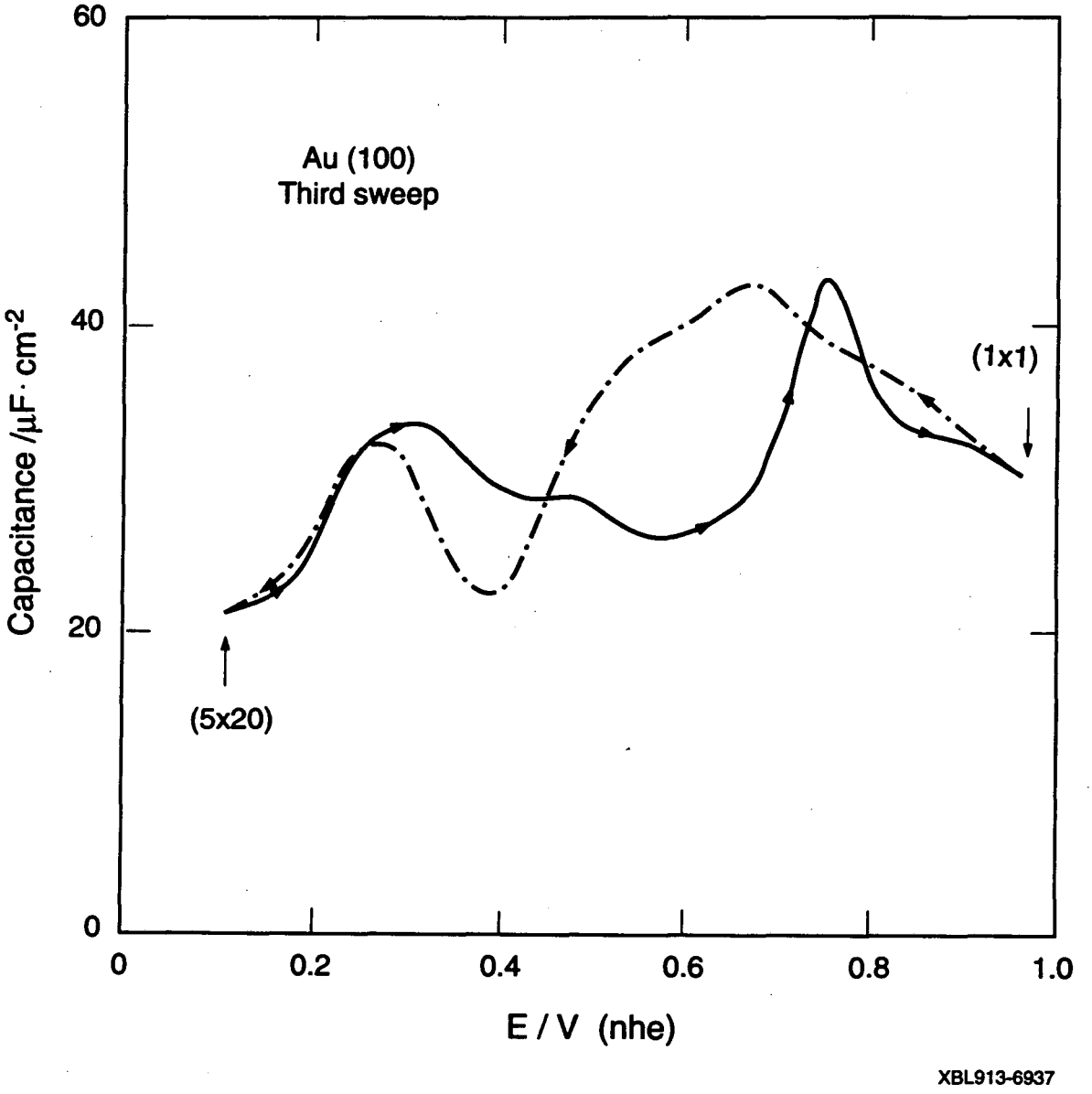
Au (100)
Third sweep
(1x1)
(5x20)
Capacitance /μF · cm-2
E / V (nhe)
60
40
20
0
0
0.2
0.4
0.6
0.8
1.0
XBL913-6937

Figure 3

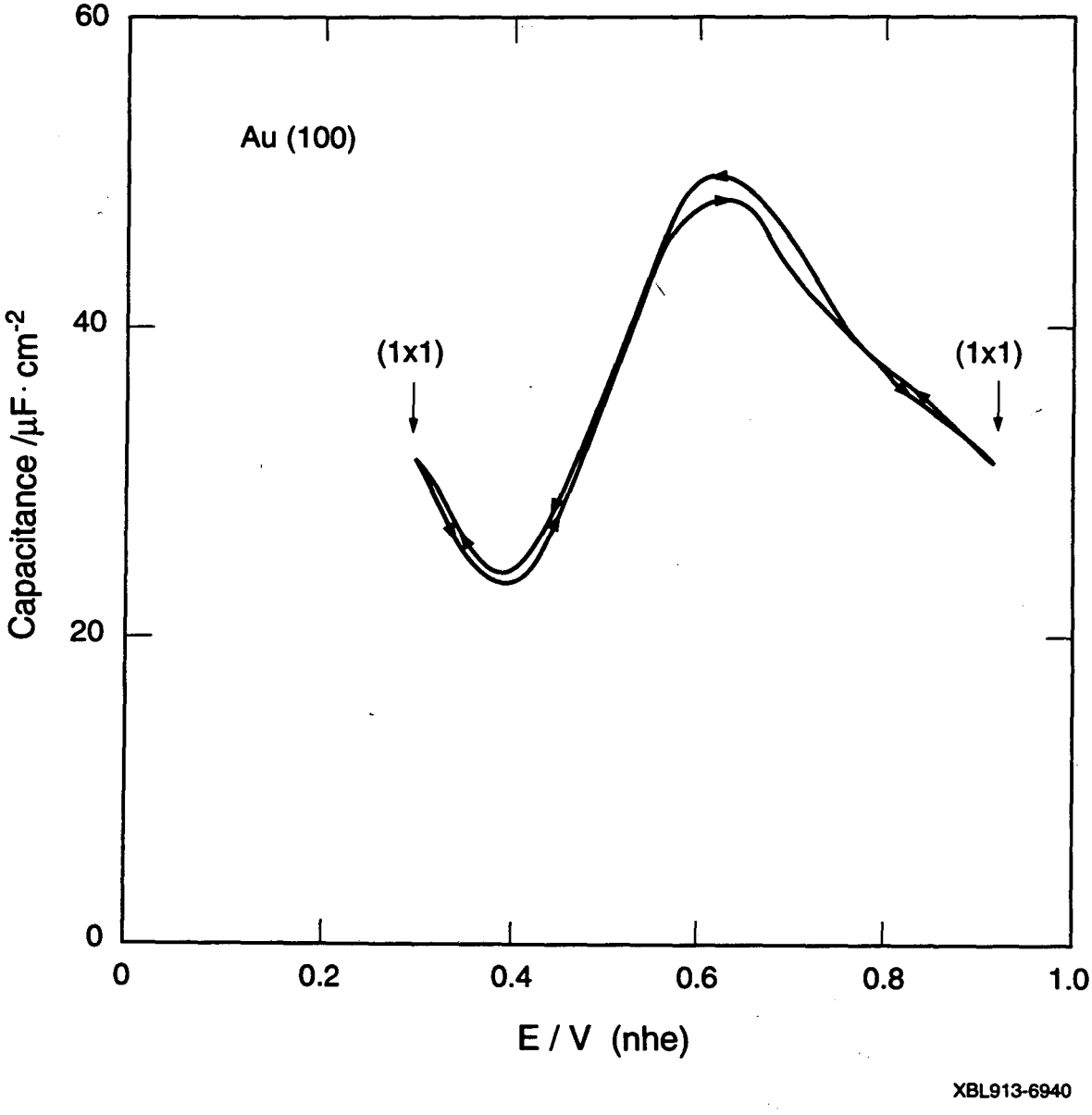
Au (100)
(1x1)
(1x1)
Capacitance /μF · cm-2
E / V (nhe)
60
40
20
0
0
0.2
0.4
0.6
0.8
1.0
XBL913-6940

Figure 4

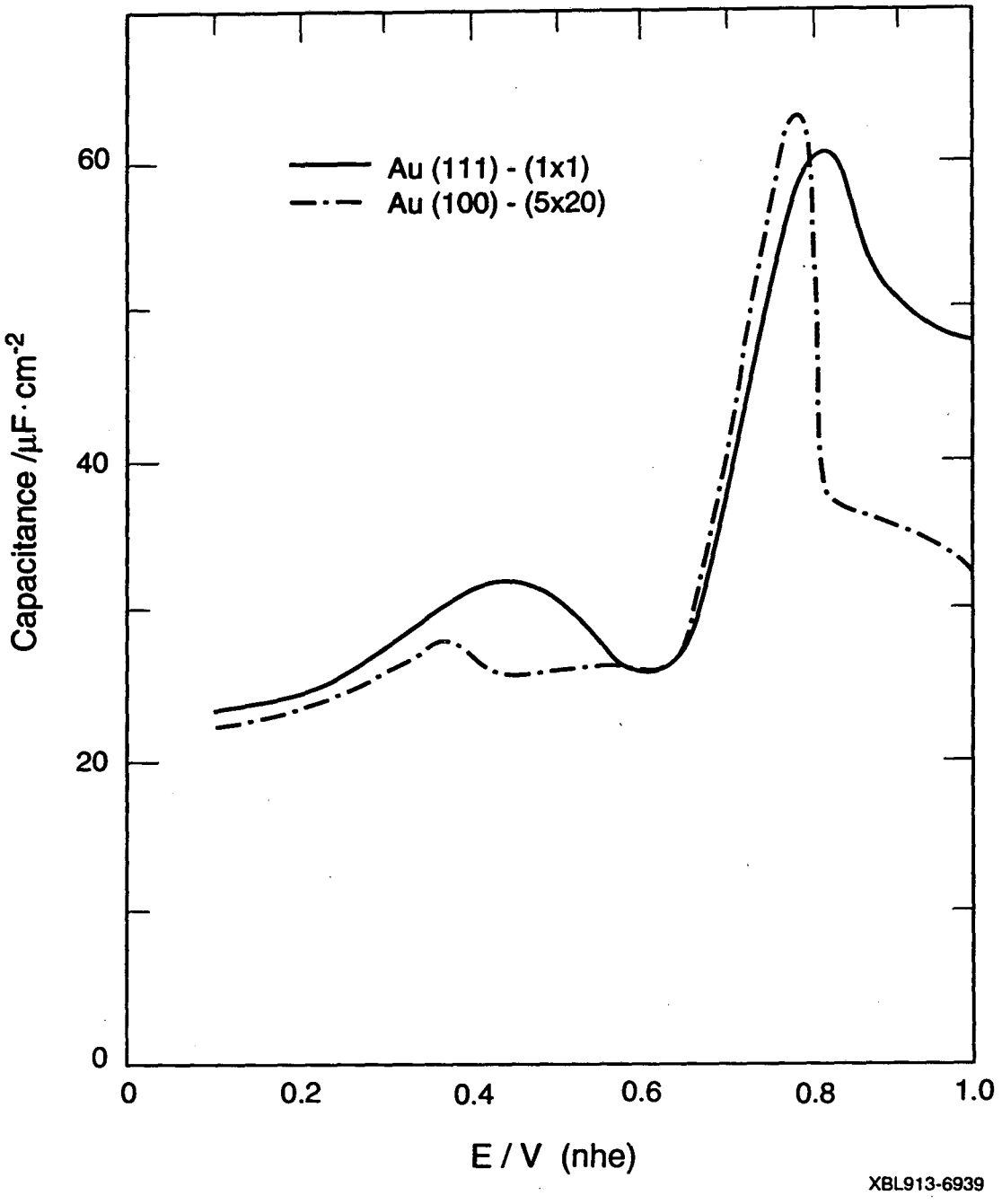
Au (111) - (1x1)
Au (100) - (5x20)
Capacitance /μF · cm-2
60
40
20
0
0
0.2
0.4
0.6
0.8
1.0
E / V (nhe)
XBL913-6939

Figure 5

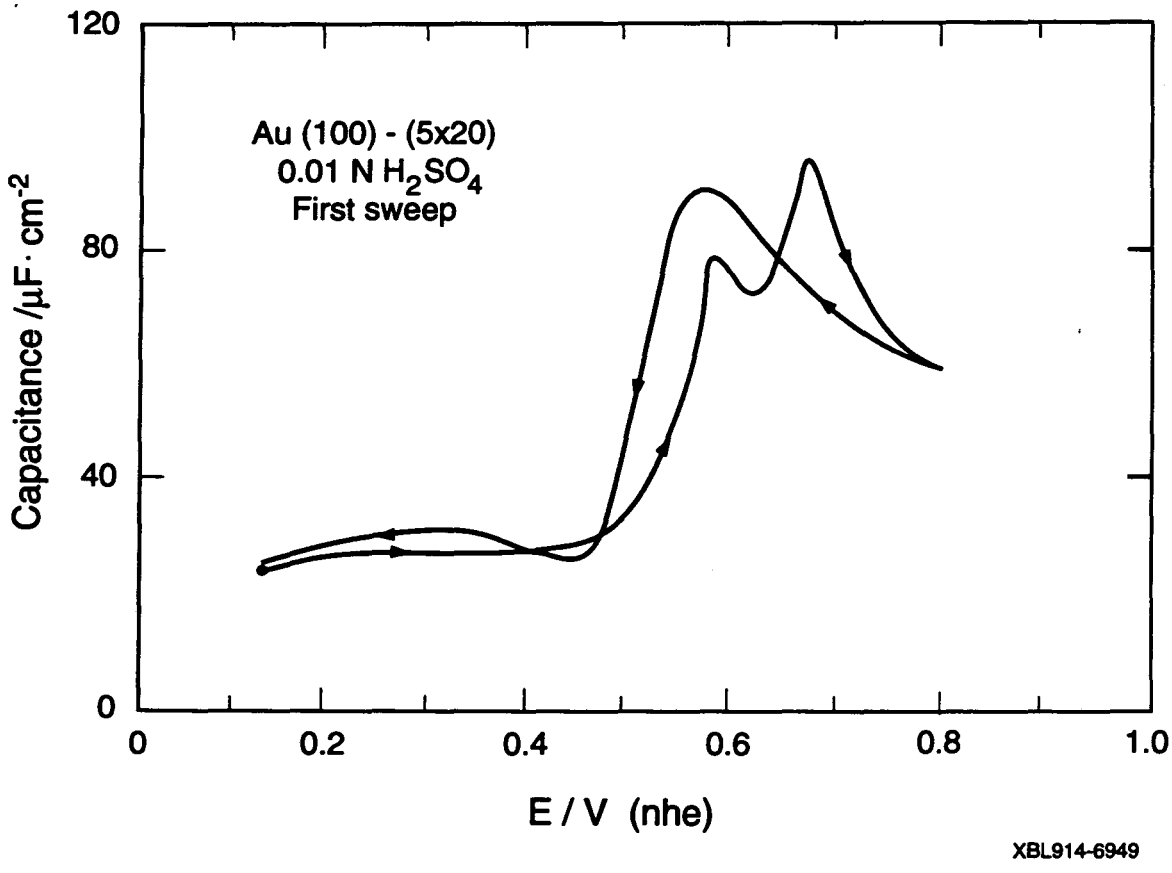
Au (100) - (5x20)
0.01 N H_2SO_4
First sweep
Capacitance /μF · cm^{-2}
120
80
40
0
0
0.2
0.4
0.6
0.8
1.0
E / V (nhe)
XBL914-6949

Figure 6

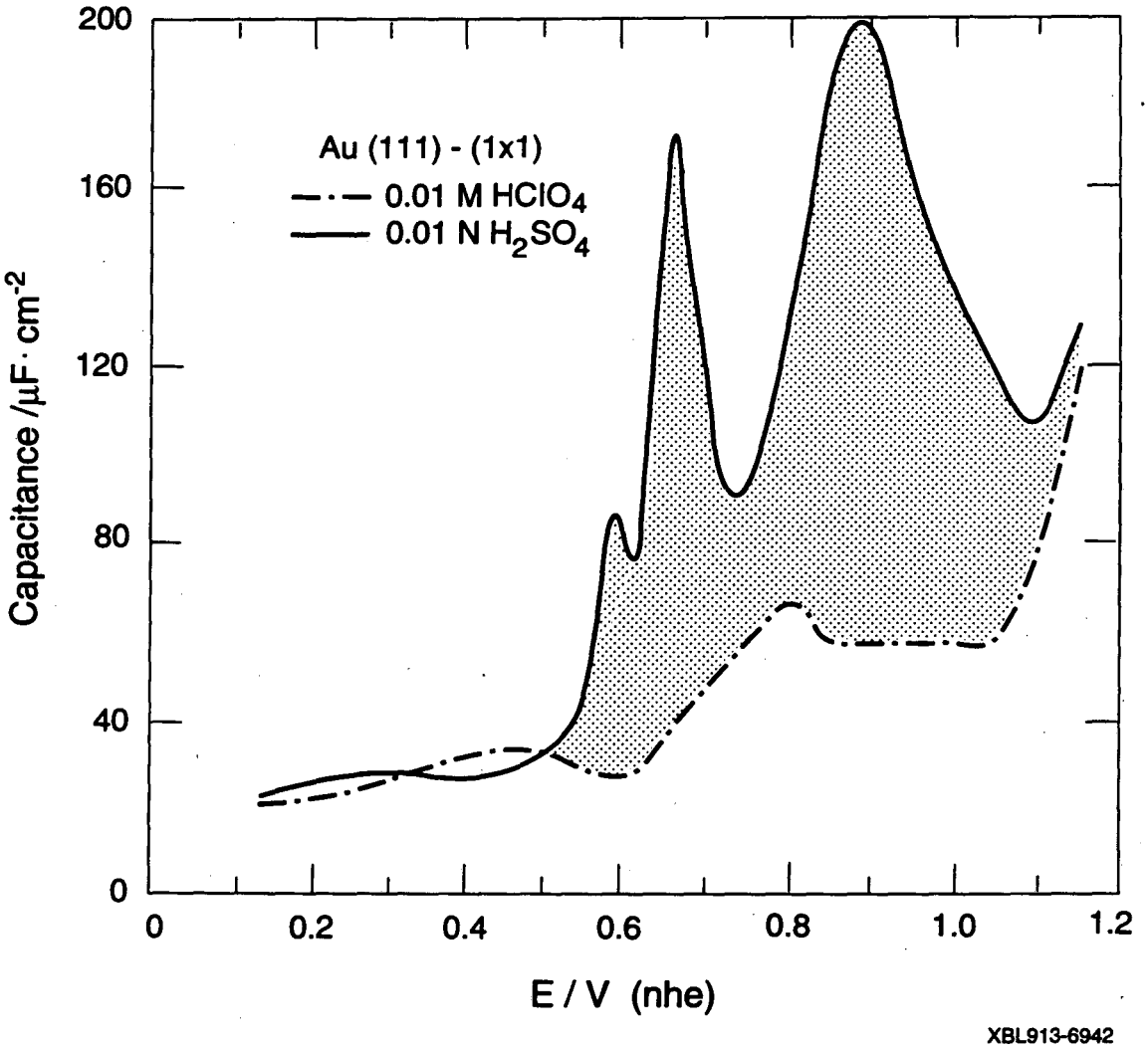
Au (111) - (1x1)
0.01 M HClO4
0.01 N H2SO4
Capacitance /μF · cm-2
200
160
120
80
40
0
0
0.2
0.4
0.6
0.8
1.0
1.2
E / V (nhe)
XBL913-6942

Figure 7

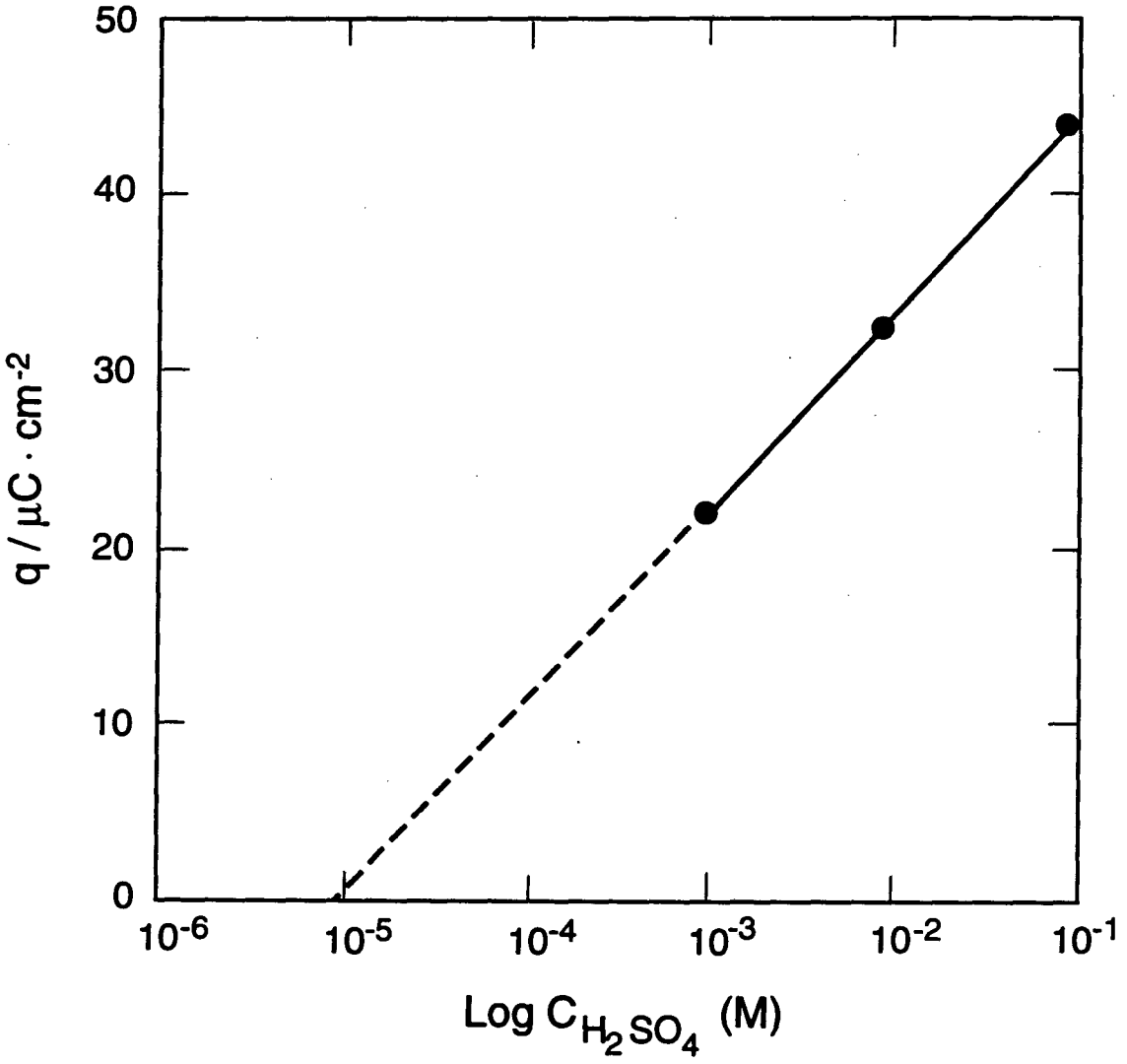

XBL913-6943

Figure 8

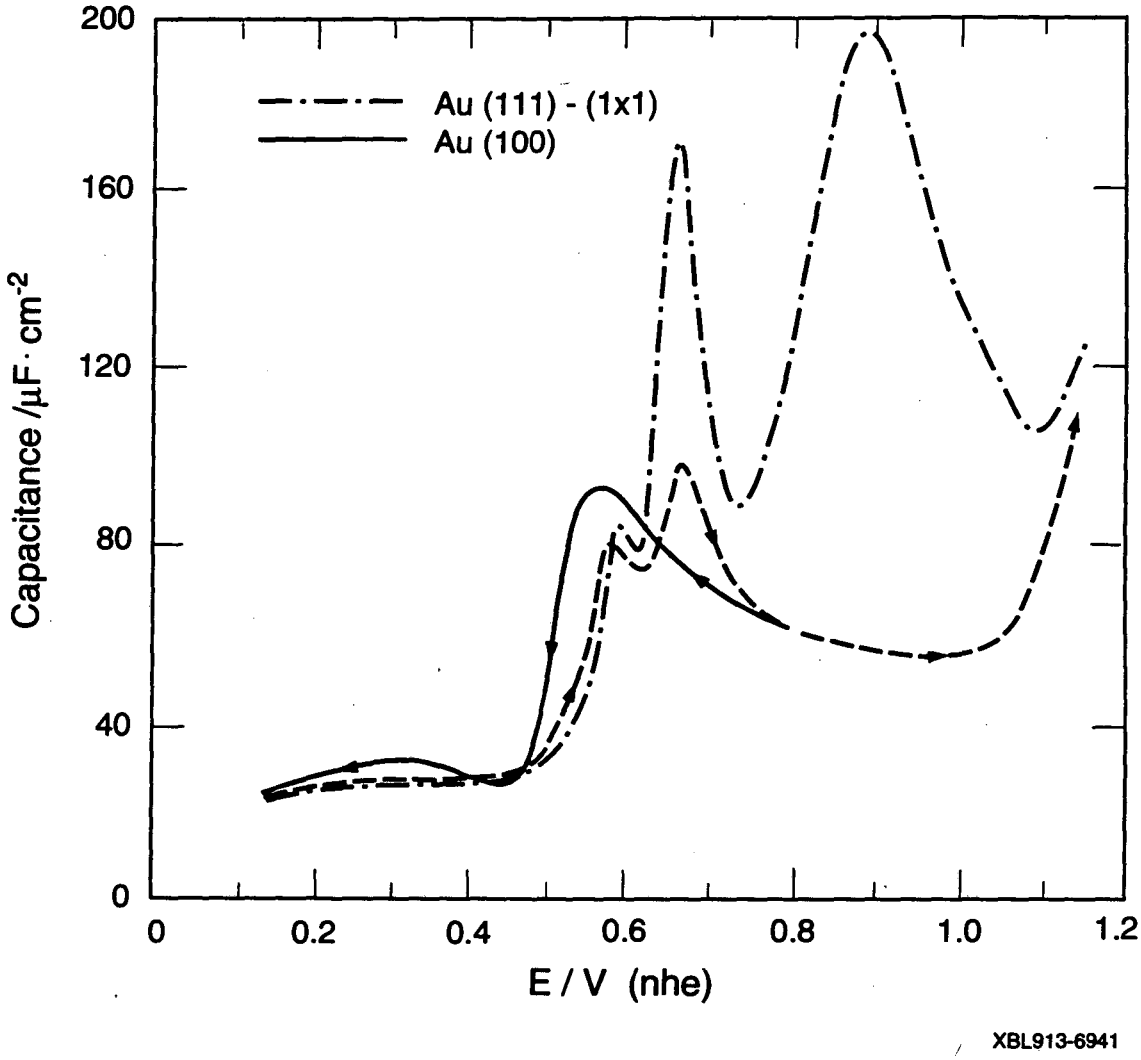
Au (111) - (1x1)
Au (100)
Capacitance /μF· cm-2
E / V (nhe)
200
160
120
80
40
0
0
0.2
0.4
0.6
0.8
1.0
1.2
XBL913-6941

Figure 9

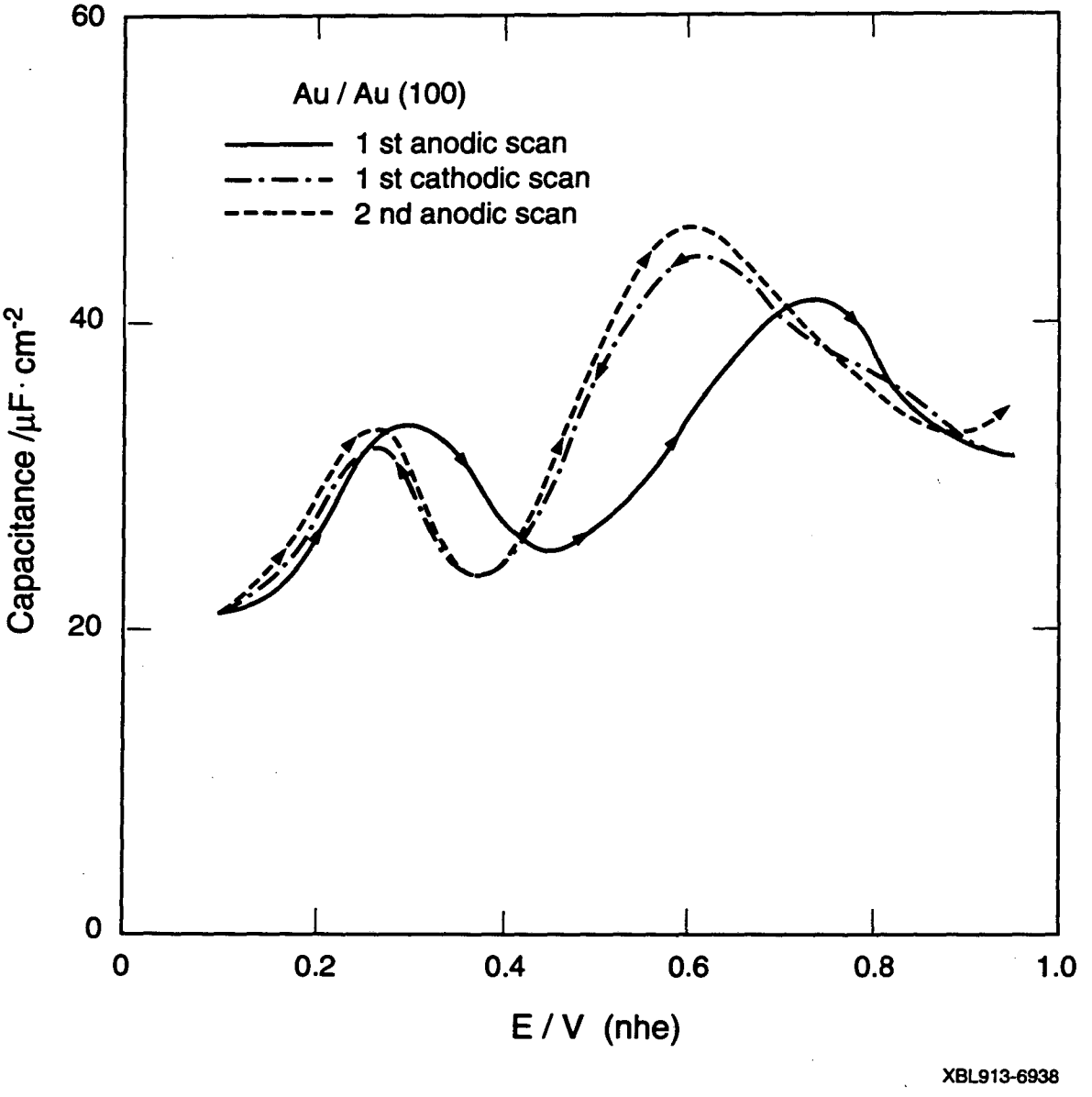
Au / Au (100)
1 st anodic scan
1 st cathodic scan
2 nd anodic scan
Capacitance /μF · cm-2
60
40
20
0
0
0.2
0.4
0.6
0.8
1.0
E / V (nhe)
XBL913-6938

Figure 10

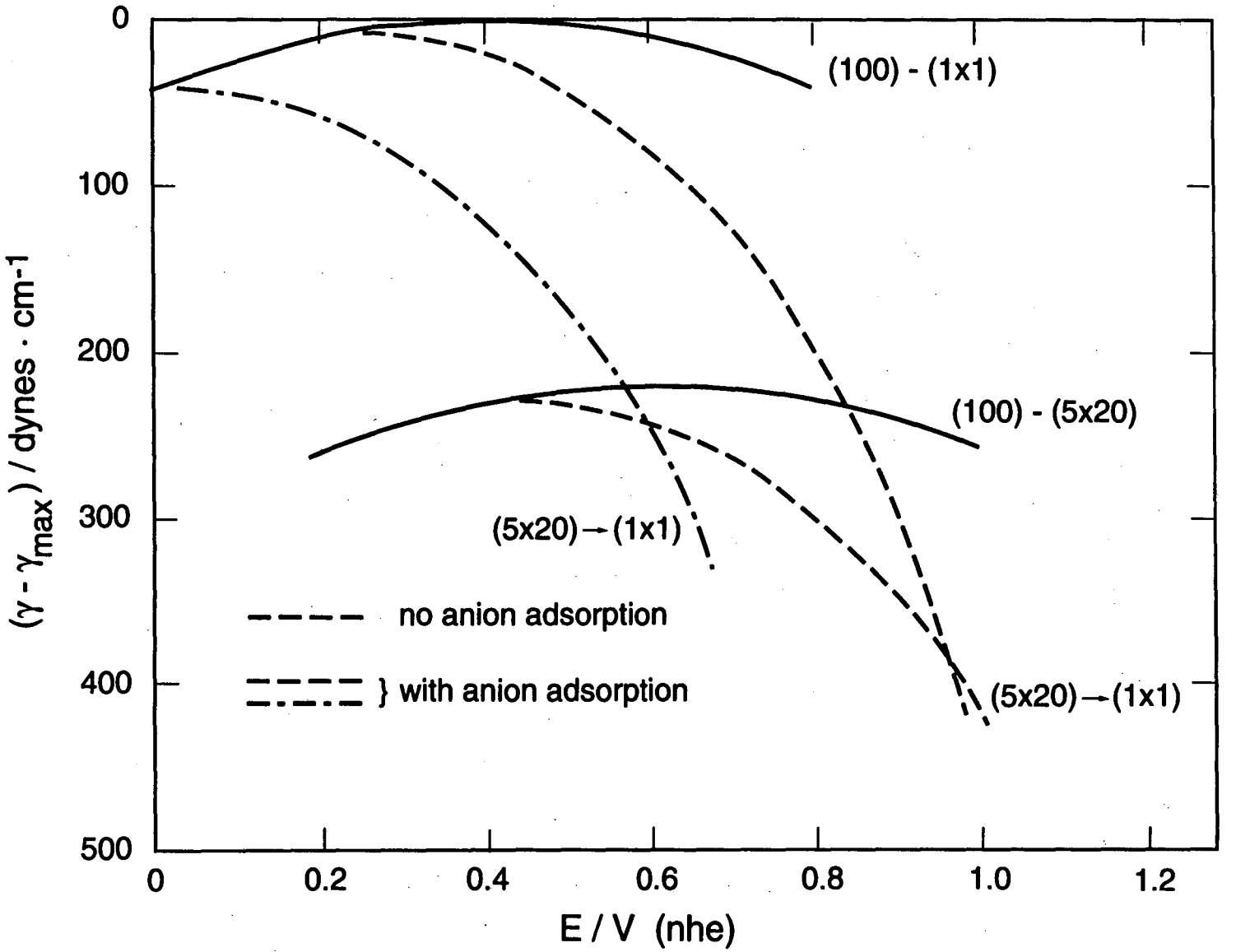

XBL914-6948

Figure 11

LAWRENCE BERKELEY LABORATORY
UNIVERSITY OF CALIFORNIA
TECHNICAL INFORMATION DEPARTMENT
BERKELEY, CALIFORNIA 94720